Geophysical Research Letters

RESEARCH LETTER
10.1029/2023GL104235

High Intra-Seasonal Variability in Greenhouse Gas Emissions From Temperate Constructed Ponds

Nicholas E. Ray[1] and **Meredith A. Holgerson**[1]

[1]Department of Ecology & Evolutionary Biology, Cornell University, Ithaca, NY, USA

Key Points:

- Constructed ponds are a net source of global greenhouse gass to the atmosphere on annual basis
- CO_2 and CH_4 exchange between ponds and the atmosphere show strong seasonal trends, with CH_4 highly variable within season
- Summertime diffusive CH_4 release dominates annual emissions budget

Supporting Information:

Supporting Information may be found in the online version of this article.

Correspondence to:

N. E. Ray,
ner35@cornell.edu

Citation:

Ray, N. E., & Holgerson, M. A. (2023). High intra-seasonal variability in greenhouse gas emissions from temperate constructed ponds. *Geophysical Research Letters*, *50*, e2023GL104235. https://doi.org/10.1029/2023GL104235

Received 20 APR 2023
Accepted 10 AUG 2023

Abstract Inland waters play a major role in global greenhouse gas (GHG) budgets. The smallest of these systems (i.e., ponds) have a particularly large—but poorly constrained—emissions footprint at the global scale. Much of this uncertainty is due to a poor understanding of temporal variability in emissions. Here, we conducted high-resolution temporal sampling to quantify GHG exchange between four temperate constructed ponds and the atmosphere on an annual basis. We show these ponds are a net source of GHGs to the atmosphere (564.4 g CO_2-eq m^{-2} yr^{-1}), driven by highly temporally variable diffusive methane (CH_4) emissions. Diffusive CH_4 release to the atmosphere was twice as high during periods when the ponds had a stratified water column than when it was mixed. Ebullitive CH_4 release was also higher during stratification. Building ponds to favor mixed conditions thus presents an opportunity to minimize the global GHG footprint of future pond construction.

Plain Language Summary Ponds are an important contributor to global greenhouse gas emissions, but there is still much uncertainty associated with global emissions estimates. To clarify this uncertainty, we investigated seasonal patterns of greenhouse gas emissions from four constructed ponds in a temperate region of the northeastern United States. We found that methane made up most of pond greenhouse gas emissions on an annual basis, leading the ponds to be a net source of greenhouse gases to the atmosphere. Methane and carbon dioxide exchange between ponds and the atmosphere followed clear seasonal patterns, with highest rates of methane release to the atmosphere during warm summer months. Ponds consumed carbon dioxide during warm months when aquatic plants were growing rapidly. We also found high variability in methane and carbon dioxide emissions over weekly time periods that was associated with whether the water column in the pond was mixed or stratified. When ponds were stratified, methane emissions were higher than during mixed conditions, possibly due to low availability of oxygen near sediments where methane is produced by micro-organisms that require low oxygen conditions. These results provide a path forward to better estimating pond greenhouse gas emissions at a global scale.

1. Introduction

Inland waters play a key role in global carbon (C) and greenhouse gas (GHG) cycling. They are a source of carbon dioxide (CO_2), methane (CH_4), and nitrous oxide (N_2O) to the atmosphere (Raymond et al., 2013; Rosentreter et al., 2021; Tian et al., 2020), but also sequester C through burial in sediments (Anderson et al., 2020; Downing et al., 2008). The smallest waterbodies (i.e., ponds) have high areal rates of both GHG emissions and C burial relative to other lentic systems (Holgerson & Raymond, 2016; Taylor et al., 2019). Globally, high areal emissions and burial rates are compounded by the sheer number of ponds (up to 3.2 billion; Downing, 2010) and waterbodies smaller than 1,000 m^2 likely contribute >5% of all global CH_4 emissions (Rosentreter et al., 2021). Constructed ponds are already prominent landscape features (e.g., 25% of all runoff in the coterminous United States is captured by a constructed pond; Renwick et al., 2006) and are likely to play an important role in both current and future global GHG and C cycling. For instance, the global number of constructed ponds is increasing as new ponds are built to provide climate-resilience in agricultural systems, manage stormwater in urban areas, provide food through inland aquaculture production, and for leisure activities (FAO, 2020; Malerba et al., 2022; Sinclair et al., 2020). Yet, GHG emission estimates from ponds at a global scale are still highly uncertain (Canadell et al., 2021; Rosentreter et al., 2021).

One major reason for this uncertainty is a lack of sufficient temporal measurements (Hofmann, 2013; Wik, Thornton, et al., 2016), as many studies investigating aquatic GHG emissions sample during only summer months, once per season, or monthly. Yet, monthly measurements of GHG fluxes from lakes and reservoirs do

not follow a smooth curve and can vary several orders of magnitude over the course of 2–3 months, particularly in the shoulder seasons when changes in the physical, chemical, and biological functions and properties of an ecosystem may yield high rates and possibly unexpected source-sink behavior (e.g., Vachon et al., 2020; Waldo et al., 2021). Temporal variability in pond GHG concentrations is high relative to larger waterbodies and may relate to intermittent periods of water column mixing and stratification (Ray et al., 2023). Specifically, stratification can lead to the accumulation of GHGs and reduced oxygen availability in bottom waters, whereas mixing can release these gases and reintroduce oxygen to the sediment-water interface (Bastviken et al., 2008; Søndergaard et al., 2023). Identifying drivers of inter- and intra- seasonal variability in pond GHG emissions is necessary to improve global GHG budgets and understand the role of constructed ponds in the future global climate system.

In this study, we quantified CO_2, CH_4, and N_2O exchange between constructed ponds and the atmosphere throughout the ice-free season in a temperate region of North America. We then identified drivers of temporal variability in flux, and combined our results with recently measured rates of C burial in adjacent constructed ponds to estimate annual emissions on a kg-CO_2-equivalent m^{-2} yr^{-1} basis.

2. Methods

2.1. Sampling Site and Scheme

We intensively sampled four constructed ponds (30 × 30 m, 2.1 m maximum depth; Figure S1 in Supporting Information S1) located at the Cornell Experimental Pond facility (42.50 N, −76.44 W) during the ice-free period of 2021. The sampled ponds are dominated by macrophytes (*Elodea canadensis*, *Ceratophyllum demersum*, *Myriophyllum sibiricum*, and to a lesser extent *Potamogeton* spp.). Fish communities consisted of sunfish (*Lepomis* spp.), fathead minnows (*Pimephales promelas*), and banded killifish (*Fundulus diaphanus*).

We collected all samples from the end of 6m floating docks, except for bubble trap samples and the first round of flux chamber samples, which were sampled from a kayak.

2.2. Weather

We collected weather data using an onsite weather station (Onset Data Loggers, Bourne, MA, USA; 10 June to 10 November), supplemented with data from the Ithaca-Tompkins Airport NOAA weather station (WBAN-94761; 1 January to 10 June and 11 November to 31 December). The onsite weather station recorded temperature, wind speed, and precipitation. The two sites had similar temperature and precipitation, though the airport weather station recorded higher wind speed. For the period that we used airport weather data, we corrected for this difference using the calculated regression of overlapping sampling dates (pond wind speed = airport wind speed × 0.523–0.291).

2.3. Dissolved Nutrients, Dissolved Oxygen, and Chlorophyll-*a* Sampling and Analysis

We measured dissolved oxygen (DO) concentrations in surface (0.25 m) and deep (1.75 m) water using an optical DO sensor attached to a Manta +35 sonde (Eureka Water Probes). We collected dissolved nutrient samples from surface water using an acid-washed syringe passed through a 0.7 µm GF/F filter into acid-washed polyethylene bottles. Samples were kept on ice in the field, and frozen until analysis. Chlorophyll-*a* (chl-*a*) samples were collected similarly with non-acid washed syringes and the GF/F filter was frozen until analysis. We collected all samples between 0900 and 1700.

We analyzed dissolved nutrients using high resolution digital colorimetry (Seal Autoanalyzer 3; SEAL Analytical) at Boston University. Dissolved NO_3^- concentrations were determined as the difference in concentration between NO_x and NO_2^-. Minimum detection limits were 0.04 µmol L^{-1} for NH_4^+, 0.02 µmol L^{-1} for NO_x, 0.02 µmol L^{-1} for NO_3^-, 0.006 µmol L^{-1} for NO_2^-, and 0.021 µmol L^{-1} for PO_4^{3-}. We analyzed chlorophyll-*a* using standard fluorometric protocols (Yentsch & Menzel, 1963).

2.4. Quantifying Stratification and Mixing

Thermistors (Onset HOBO pendants) at the pond surface (0.10 m) and bottom (1.95 m) logged temperature every 10 min. We calculated water density from water temperature using the *rLakeAnalyzer* package (Read

et al., 2011; assuming salinity = 0), and considered the pond mixed if the density gradient between the sensors was <0.287 kg m^{-3} m^{-1} (Holgerson et al., 2022).

2.5. Diffusive Flux Sampling

We used floating chambers (18.93 L; 0.071 m^2 cross sectional area; Dacey & Klug, 1979) to measure diffusive GHG flux between ponds and the atmosphere approximately biweekly from 5 April to 10 November (n = 16 sampling events). On each sampling date, we deployed two floating chambers on each pond. A luer-lock valve on the chamber was left open for 10 minutes following chamber deployment to equilibrate with atmospheric pressure. We collected 45 ml samples from the chamber every 30–40 min over ~2 hr (n = 5 sampling points), which we stored in 22 ml evacuated glass vials.

2.6. Ebullitive Flux Sampling

We deployed three bubble traps across a transect in each pond to measure ebullition rates from April 14 to November 10 (n = 23 sampling events). We constructed traps from funnels (cross sectional area 0.059 m^2) attached to 500 ml plastic graduated cylinders (similar to Wik et al., 2013). Around each cylinder, we loosely attached a square piece of wood and foam insulation to maintain buoyancy while allowing the cylinder to slide up and down. We deployed chambers by inverting them and fully submerging them, before flipping them and ensuring they were full of water with no headspace. We recorded the volume of accumulated gas collected in the bubble traps at least weekly in the summer, and every 2–3 weeks in spring and fall when less ebullition occurred. One trap in each pond was equipped with a sampling port to collect samples for GHG analysis. We collected GHG samples each time gas volume was measured, except when not enough volume accumulated in the trap (17/92 sampling events) or when the valve was found open prior to sampling (22/92 sampling events). On these occasions, we used the mean CH_4 concentration from other ponds sampled on the same date or the mean value of the preceding and following week if no ponds were sampled. In early spring and fall when little bubbles were produced, we took the average CH_4 concentration from all traps over all sampling times.

2.7. Analysis of Gas Concentrations and Flux Calculation

We analyzed gas samples using a Shimadzu GC 2014 equipped with a flame ionization detector, methanizer, and electron capture detector. We estimated diffusive flux as the linear change in gas concentration over time $\left(\frac{\Delta ppm}{\Delta hr}\right)$. We considered fluxes with $R^2 \geq 0.65$ as significant and those with $R^2 < 0.65$ as non-significant, and equal to zero (33/119 for CO_2, 10/115 for CH_4, and 83/119 for N_2O; Prairie, 1996; Ray & Fulweiler, 2021). We converted non-zero fluxes from $\frac{\Delta ppm}{\Delta hr}$ to $\frac{\Delta atm}{\Delta hr}$ by multiplying by the atmospheric pressure (atm) during the incubation divided by 1,000,000 to remove the ppm conversion. Diffusive fluxes were calculated similarly to DelSontro et al. (2016):

$$\text{Diffusive Flux}\left(\text{mmol m}^{-2}\,\text{hr}^{-1}\right) = \frac{\left(\frac{\Delta atm}{\Delta hr}\right) \times \text{Chamber Volume}\,(L) \times \frac{1000\,\text{mmol}}{1\,\text{mol}}}{R\left(L\,\text{atm K}^{-1}\,\text{mol}^{-1}\right) \times \text{Temperature}\,(K) \times \text{Area}(m^2)} \quad (1)$$

Where R is the universal/ideal gas constant (0.082056 L atm K^{-1} mol^{-1}) and K is the air temperature (K) at the incubation start.

Ebullitive fluxes were calculated similarly to Wik et al. (2013):

$$\text{Ebullitive Flux}\left(\text{mmol m}^{-2}\,\text{hr}^{-1}\right) = \frac{[CH_4] \times \text{Bubble Volume}(L) \times \frac{1\,\text{mmol}}{1000\,\mu\text{mol}}}{\text{Area}\,(m^2) \times \text{Time(hr)} \times V_m} \quad (2)$$

Where $[CH_4]$ is the concentration of CH_4 in the trapped bubble (μL L^{-1}), and V_m is the molar volume of gas at standard conditions (22.4 L mol^{-1}).

2.8. Identifying Drivers of Flux Variability

We used a multivariate approach to identify the best predictors of temporal variability in fluxes. There was substantial correlation among mean, maximum, and minimum air temperature and among dissolved nutrient

concentrations (Table S1 in Supporting Information S1). Thus, we use mean air temperature to represent temperature measurements and NH_4^+ to represent dissolved nutrients.

For each diffusive flux, we constructed a linear mixed model that included mean daily air temperature, mean wind speed, total daily precipitation, NH_4^+ concentration, and chlorophyll-*a* concentration (all scaled) as fixed effects, and "pond" as a random effect to account for repeated measurements via the *lme4* package (Bates et al., 2015). We compared all possible combinations of these fixed effects using corrected Aikake Information Criterion (AICc) via the *MuMin* package in R (Barton, 2020). We considered the best model to have the lowest AICc and any models within 2 ΔAICc to be well supported (Burnham & Anderson, 2002; Tables S2–S4 in Supporting Information S1). We report AICc values for the base model, the null model, the best model, and all models within 2 ΔAICc of the best model. We repeated this approach for ebullitive CH_4 flux, using the mean air temperature and wind over the sampling period, total precipitation over that period, and NH_4^+, and chl-*a* concentrations during the sampling period (i.e., samples collected between ebullition sampling days). Since nutrients and chl-*a* were not collected during each ebullitive flux sampling period, several dates were not included in model selection (model $n = 52$).

We excluded pond stratification status from multivariate models as it was associated with mean temperature (logit regression $p < 0.001$; Figure S4 in Supporting Information S1). To test if pond stratification influenced GHG flux, we created mixed effects models with stratification as a fixed effect and pond as a random effect and used pairwise least square means tests via the *emmeans* package (Lenth, 2018). To compare ebullitive flux during periods of mixing/stratification, we determined whether there was a mixing event during the bubble accumulation period and classified that period as "Stratified" if no mixing occurred or ">1 Mixed Day" if there was a mixing event.

2.9. Calculating an Annual GHG Budget

We estimated monthly emissions by integrating the area between the mean flux rate and zero for each GHG using the AUC command in the *DescTools* package in R (Signorell et al., 2017), using a trapezoidal method for diffusive fluxes and step method for ebullitive fluxes. We converted from molar rates to g CO_2-equivalents using used 100-year global warming potential values of 27.2 for CH_4 and 298 for N_2O. We assumed flux was constant over a 24-hr period. To calculate a net GHG budget, we subtracted an annual organic C (OC) burial of 245.8 g CO_2 m^{-2} estimated from 22 adjacent experimental ponds (mean burial rate: 67.1 g OC m^{-2} yr^{-1}; Holgerson et al., 2023).

3. Results

3.1. Weather and Pond Conditions

Weather conditions followed typical temperate patterns (Figures S2a–S2c in Supporting Information S1). Dissolved nutrient concentrations in surface water were low throughout the year with no discernible patterns (0.39 ± 0.02 μmol NH_4^+ L^{-1}; mean ± SE; 0.26 ± 0.04 μmol NO_x L^{-1}; 0.07 ± 0.04 μmol PO_4^{3-} L^{-1}). Ponds were highly productive due to substantial macrophyte growth beginning in late spring, when DO was supersaturated and concentrations were higher in bottom waters near to the macrophytes (Figure S2d in Supporting Information S1). Macrophyte growth slowed in mid-July when they had grown near to the surface and DO became undersaturated in bottom waters while surface waters maintained ~100% saturation until mid-September, when macrophytes began to senesce and the water column mixed. Snorkel surveys revealed 100% vegetation cover of the pond centers in August. Chl-*a* concentrations were low (3.70 ± 0.21 μg L^{-1}) throughout the year.

Ponds were generally mixed throughout the spring (100% of measured days in April and 87% of days in May; Figure S3 in Supporting Information S1) and stratified during summer (mixing only occurred on 43%, 37%, and 16% of days in June, July, and August respectively). The ponds mixed frequently in the fall (94% of days in September, and all days in October and November).

3.2. Annual Emissions Patterns

Diffusive GHG exchange between the constructed ponds and atmosphere followed a clear seasonal pattern, with little exchange until late spring when ponds became a CO_2 sink (May mean flux -0.48 ± 0.16 mmol CO_2

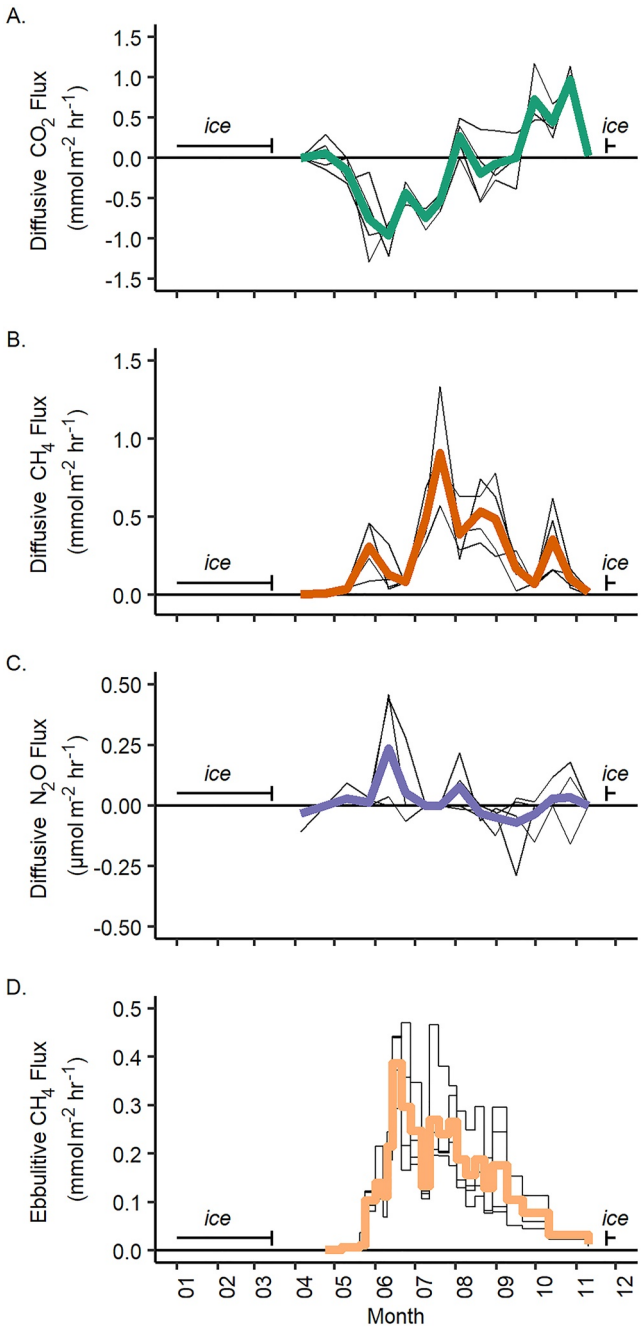

Figure 1. Diffusive fluxes of (a) carbon dioxide, (b) methane, and (c) nitrous oxide ($n = 16$ dates), and (d) ebullitive flux from constructed ponds on an annual basis ($n = 23$ dates). Thin black lines indicate flux from each replicate pond and the thicker, colored lines represent the mean flux ($n = 4$). Fluxes above the zero line indicate release to the atmosphere. Those below the line indicate uptake by the pond.

m^{-2} hr^{-1}) and remained so throughout the summer (June and July mean flux −0.67 ± 0.08 mmol CO_2 m^{-2} hr^{-1}) until the transition to fall (August and September) when they bounced between source-sink behavior (Figure 1a). The ponds released CO_2 in October and November at rates similar in magnitude to the summer CO_2 sink period (October and November mean flux 0.47 ± 0.10 mmol CO_2 m^{-2} hr^{-1}). The ponds were always a source of CH_4 to the atmosphere via diffusion (Figure 1b), with low emissions in spring (April and May mean flux 0.11 ± 0.03 mmol CH_4 m^{-2} hr^{-1}) followed by a rapid increase in emission mid-summer (July mean flux 0.71 ± 0.11 mmol CH_4 m^{-2} hr^{-1}) that slowly declined until ice formation. The best model to predict diffusive CO_2 flux included mean daily temperature ($\beta = -0.28$; SE = 0.05) and [NH_4^+] ($\beta = 0.36$; SE = 0.05; $p < 0.01$; marginal $R^2 = 0.60$; Table S2 in Supporting Information S1), while the best model to predict diffusive CH_4 flux was temperature alone ($\beta = 0.06$; SE = 0.01; $p < 0.01$; marginal $R^2 = 0.49$; Table S3 in Supporting Information S1). N_2O emissions bounced between release and uptake throughout the year (Figure 1c), and none of the variables we measured predicted N_2O flux (Table S4 in Supporting Information S1).

Bubble production was highest in late spring (Figure S5 in Supporting Information S1). Bubble CH_4 concentration varied throughout the year (2.0%–49.5% CH_4; Figure S5 in Supporting Information S1) with lowest concentrations generally coinciding with the highest rates of bubble production (linear regression, $F = 5.19$, $R^2 = 0.20$, $p = 0.04$). Like diffusive emissions, ebullitive CH_4 emissions followed a clear seasonal pattern (Figure 1d), best predicted by mean temperature ($\beta = 0.10$; SE = 0.01) and [NH_4^+] ($\beta = -0.06$; SE = 0.01; $p < 0.01$; marginal $R^2 = 0.66$; Table S5 in Supporting Information S1). Ebullitive emissions were low in spring before a rapid increase in mid-May, when mean ebullitive flux increased from 0.01 ± 0.01 mmol CH_4 m^{-2} hr^{-1} between May 6–20 to a peak emission rate of 0.39 ± 0.04 mmol CH_4 m^{-2} hr^{-1} between June 10–14. Following this peak, CH_4 ebullition steadily declined before returning to springtime levels in mid-fall (0.03 ± 0.00 mmol CH_4 m^{-2} hr^{-1} the week ending October 11).

3.3. Mixing Status as a Predictor of Temporal Variability in Greenhouse Gas Fluxes

Diffusive CO_2 and CH_4 fluxes followed seasonal temperature patterns, but also displayed high variability within short time frames. For example, the difference in diffusive CH_4 flux between June 24 (0.09 ± 0.02 mmol CH_4 m^{-2} hr^{-1}) and July 9 (0.49 ± 0.06 mmol CH_4 m^{-2} hr^{-1}) was comparable to the difference between mean spring (April & May; 0.11 ± 0.04 mmol CH_4 m^{-2} hr^{-1}) and summer (June—August; 0.43 ± 0.05 mmol CH_4 m^{-2} hr^{-1}) fluxes. Mean daily temperature only differed 3.24°C between these two sampling events (average mean daily temperature in spring and summer were 10.2 and 21.0°C respectively), indicating temperature alone is not responsible for the observed differences in flux. Rather, mixing may explain these results as ponds were mixed on June 24, and stratified on July 9.

We compared diffusive exchange measured when the water column was stratified ($n = 20$ samples) and mixed ($n = 36$) and found that CO_2 fluxes were significantly higher, and on average ponds were a source of CO_2 to the atmosphere, when the water column was mixed (0.096 ± 0.096 mmol m^{-2} h^{-1}) compared to when ponds were stratified, and served as a CO_2 sink (−0.451 ± 0.101 mmol m^{-2} h^{-1}; least square means, $df = 52$, t-ratio = 3.635, $p < 0.001$; Figure 2a). The opposite was true for diffusive CH_4 fluxes—emissions during periods of stratification (0.504 ± 0.072 mmol m^{-2} h^{-1}) were

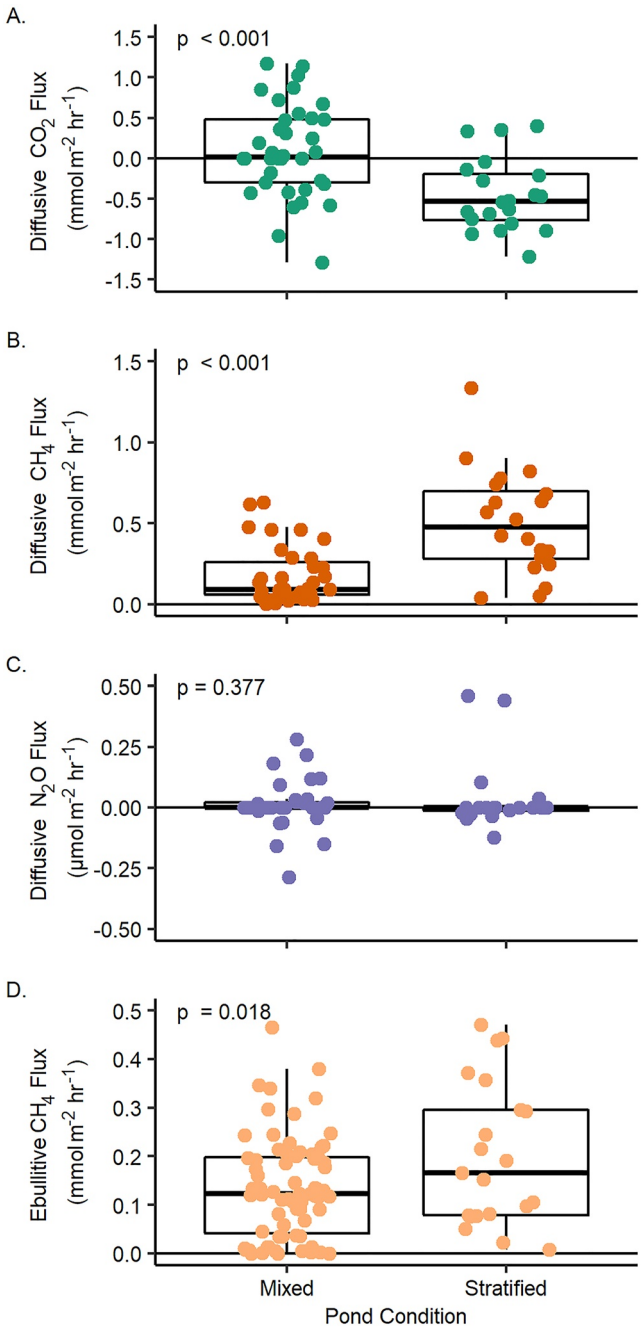

Figure 2. Diffusive fluxes of (a) carbon dioxide, (b) methane, and (c) nitrous oxide when ponds were mixed or stratified during sampling. (d) Ebullitive CH_4 fluxes when ponds were fully stratified ("Stratified") or experienced at least one mixing event ("Mixed") during the gas accumulation period. *P*-values indicate results of least-square means tests, points indicate individual flux measurements, the solid line in each box indicates the median and the box edges indicate the 25th and 75th percentiles. Fluxes above the zero line indicate release to the atmosphere. Those below the line indicate uptake by the pond.

more than twice as high as periods of mixing (0.177 ± 0.030 mmol m^{-2} h^{-1}; least square means test, $df = 51.1$, t-ratio = −4.052, $p < 0.001$; Figure 2b). N_2O flux did not differ between periods of mixing (0.010 ± 0.016 μmol m^{-2} h^{-1}) or stratification (0.039 ± 0.033 μmol m^{-2} h^{-1}; least square means test, $df = 51.7$, t-ratio = −0.891, $p = 0.377$; Figure 2c).

Ebullitive CH_4 flux was higher when the water column was stratified the entire period of bubble accumulation (0.202 ± 0.032 mmol m^{-2} h^{-1}) compared to when mixing occurred at least once during this accumulation period (0.135 ± 0.012 mmol m^{-2} h^{-1}; least square means test, $df = 87.1$, t-ratio = −2.410, $p = 0.018$; Figure 2d).

3.4. Annual GHG Budget

Annually, we estimate the constructed ponds were a sink for 0.47 mol CO_2 m^{-2} yr^{-1} and released 1.90 mol CH_4 m^{-2} yr^{-1} (1.32 mol CH_4 m^{-2} yr^{-1} via diffusive flux and 0.59 mol CH_4 m^{-2} yr^{-1} via ebullitive flux) and 0.05 μmol N_2O m^{-2} yr^{-1}. In CO_2-equivalents, this equates to release of 810.3 g CO_2-eq m^{-2} yr^{-1} (Figure 3). Despite burial of 245.8 g CO_2-eq m^{-2} yr^{-1} (Holgerson et al., 2023), the ponds were a net source of GHGs to the atmosphere on an annual basis (net 564.4 g CO_2-eq m^{-2} yr^{-1}; Figure 3). Diffusive CH_4 flux drove total emissions, contributing 71% of GHG release in terms of g CO_2-eq m^{-2} yr^{-1}. Summertime diffusive CH_4 emissions were particularly important, with diffusive CH_4 emissions in July (194.6 g CO_2-eq m^{-2} $month^{-1}$) and August (149.9 g CO_2-eq m^{-2} $month^{-1}$) nearly equal to annual CH_4 ebullitive flux (256.5 9 g CO_2-eq m^{-2} yr^{-1}).

4. Discussion

Temporal variability is a major uncertainty in pond GHG budgets. Here, we used a high-resolution sampling campaign to demonstrate that temperate constructed ponds are a net source of GHGs to the atmosphere. On an annual basis total GHG emissions—in g CO_2-eq m^{-2} yr^{-1}—are driven by temporally variable diffusive CH_4 flux. While GHG exchange with the atmosphere followed clear seasonal patterns, we recorded high intra-seasonal variability in both CO_2 and CH_4 fluxes that was linked with temperature and water column stratification. Importantly, seasonal patterns and intra-seasonal variability in GHG fluxes were synchronous across the four ponds sampled. These results demonstrate that external processes can control inter- and intra-seasonal variability in pond GHG fluxes.

Diffusive CO_2 fluxes followed a clear seasonal pattern, with net CO_2 consumption from late spring through summer and net CO_2 release in the fall, similar to previously reported seasonal CO_2 emissions patterns from temperate ponds and lakes (e.g., Baliña et al., 2023; Natchimuthu et al., 2014; Riera et al., 1999). We see two, not mutually exclusive explanations for this seasonal cycle. First, the ponds exhibited rapid macrophyte growth and CO_2 uptake in spring and summer, whereas in fall, respiration from senescence outpaces production and ponds release CO_2. The relationships between temperature and [NH_4^+] and diffusive CO_2 flux fit with this seasonal biological process—during warm seasons, plants take NH_4^+ from the water column to support growth and primary production (Ozimek et al., 1993), leading to undersaturation of water column CO_2. During cooler seasons, decomposition releases CO_2 and NH_4^+ to the water column (Pieczyńska, 1993). The second explanation considers pond mixing status. CO_2 was released during the fall months when ponds were mixed and was consumed during summer months when ponds were stratified.

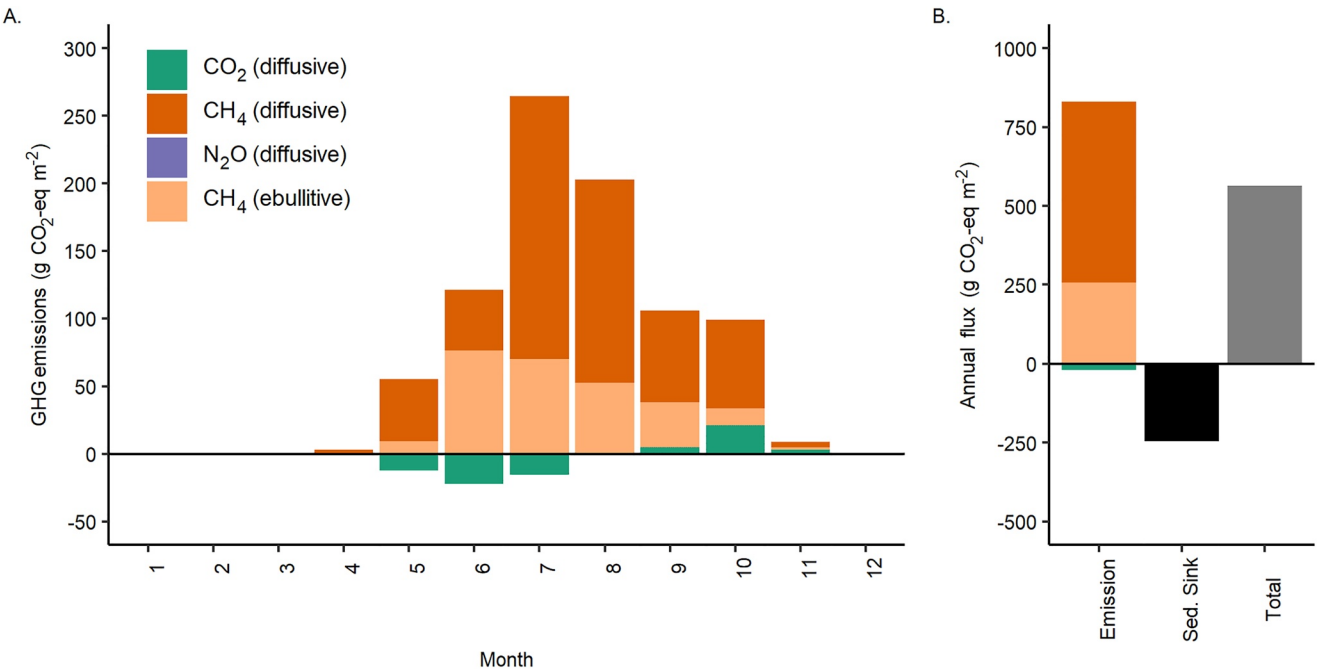

Figure 3. Greenhouse gas emissions (in g CO_2-eq m^{-2}) from temperate constructed ponds on (a) a monthly and (b) annual basis. The sediment CO_2 sink value is from Holgerson et al. (2023). The contribution of nitrous oxide (N_2O) emissions is too small to be seen on the graph.

During mixing, CO_2 produced during benthic respiration can vent to the atmosphere (Eugster et al., 2003) and NH_4^+ produced in the benthos is more likely to be available in surface waters (MacIntyre et al., 2006). Untangling the role of macrophyte growth or mixing dynamics on regulating CO_2 emissions is further complicated by the physical structure of dense macrophyte communities promoting stratification (Andersen et al., 2017). Resolving the independent and synergistic effects of macrophytes and mixing is an important next step to better constrain annual emissions from ponds.

Both diffusive and ebullitive CH_4 fluxes tracked temperature (Figure S6 in Supporting Information S1) with highest emissions during the warmest months, similar to previous observations (e.g., Aben et al., 2017; Davidson et al., 2018; Wik et al., 2014). Yet, summertime CH_4 emissions also displayed high variability over short timeframes, which cannot be explained by temperature alone. Rather, variability in CH_4 flux was likely driven by pond stratification dynamics—both diffusive and ebullitive CH_4 emissions were higher during periods of stratification and lower during periods of mixing. Stratification affects the extent to which CH_4 accumulating in bottom waters is stored, oxidized, or diffused to surface waters (Bastviken et al., 2008; Søndergaard et al., 2023). Storage will be higher if waters are anoxic and stratified, whereas mixing will release accumulated CH_4 to surface waters and the atmosphere (Søndergaard et al., 2023) and simultaneously reintroduce oxygen to bottom waters (Andersen et al., 2017). We observed the highest CH_4 fluxes in July and August, when ponds were warm and mostly stratified, and benthic DO was undersaturated. We propose that despite stratification storing CH_4 in bottom waters, diffusive CH_4 fluxes were high due to diffusion across a relatively shallow water column, and may have been promoted by partial mixing events and internal turbulence. We suspect that when we sampled ponds in the mixed state, we missed the short-term pulses of accumulated CH_4 release, instead capturing lower rates of CH_4 emission. Fluxes were lower in May and June, when the ponds mixed more and benthic DO was higher (Figure S2d in Supporting Information S1). The negative relationship between ebullitive CH_4 emissions and [NH_4^+] may also result from stratification. Increased macrophyte density and height strengthens stratification, may lead to low surface [NH_4^+] due to plant uptake, and promotes the accumulation of CH_4 in bottom waters, which likely increases ebullition. In contrast, mixing increases aerobic conditions that favor NH_4^+ production from aerobic decomposition, while also potentially promoting methanotrophy and limiting methanogenesis. Stratification status has been linked with pond CH_4 emissions previously: van Bergen et al. (2019) report highest CH_4 emissions in summer months when an urban pond became stratified during the daytime and mixed at night compared to months when the pond was consistently mixed.

The annual GHG budget for the constructed ponds was largely driven by CH_4 emission and C burial, with negligible influence from CO_2 and N_2O. Importantly, more than twice as much CH_4 was released to the atmosphere via diffusion than ebullition. This contrasts global syntheses of lentic CH_4 emissions where ebullition has been suggested as the dominant CH_4 emission pathway (e.g., Aben et al., 2017; Wik, Varner, et al., 2016; though other work indicates the importance of ebullition varies dramatically across systems, e.g., Deemer & Holgerson, 2021). This disparity may be associated with differences in mixing dynamics in ponds compared to lakes. In the intermittently mixed ponds measured here, diffusive and ebullitive emissions were similar under mixed conditions (mean flux of 0.177 and 0.123 mmol CH_4 m^{-2} hr^{-1} respectively), but diffusive fluxes were more than twice as high as ebullitive fluxes during periods of stratification (0.504 and 0.202 mmol CH_4 m^{-2} hr^{-1} respectively). Thus, a better understanding of how pond mixing regimes influence ebullitive and diffusive CH_4 fluxes appears important for reducing uncertainty in pond CH_4 emissions. Similarly, studies should be conducted in ponds dominated by phytoplankton and in other climatic regions to test if the patterns observed here hold.

Improving our understanding of mixing dynamics in ponds is necessary to accurately upscale global aquatic GHG emissions, particularly as periods of stratification increase under global warming and stilling (Jane et al., 2023; Woolway et al., 2019). More stratification is likely to enhance CH_4 emissions from inland waters (Jansen et al., 2022), an increase that will be compounded by greater CH_4 production in the benthos associated with faster microbial metabolism (Aben et al., 2017), further exacerbating anthropogenic CH_4 emissions and increasing the contribution of small waterbodies to global CH_4 emissions inventories. Identifying strategies to convert CH_4 to CO_2 in constructed ponds, or designing constructed ponds to favor persistent mixed conditions, presents an opportunity to reduce their GHG footprint at the global scale.

Data Availability Statement

The data from this study can be accessed via the Figshare repository (https://doi.org/10.6084/m9.figshare.22626862.v1).

Acknowledgments
We thank Benj Sterret, Chelsea Russ, Danielle Preston, and Meredith Theus for assistance collecting samples, Brian Brown for assistance constructing flux chambers and bubble traps, and Kim and Jed Sparks for assistance processing greenhouse gas samples. This project was partly funded by the New York State Water Resources Institute and the National Science Foundation (Grant 2143449).

References

Aben, R. C. H., Barros, N., Van Donk, E., Frenken, T., Hilt, S., Kazanjian, G., et al. (2017). Cross continental increase in methane ebullition under climate change. *Nature Communications*, *8*(1), 1682. https://doi.org/10.1038/s41467-017-01535-y

Andersen, M. R., Sand-Jensen, K., Iestyn Woolway, R., & Jones, I. D. (2017). Profound daily vertical stratification and mixing in a small, shallow, wind-exposed lake with submerged macrophytes. *Aquatic Sciences*, *79*(2), 395–406. https://doi.org/10.1007/s00027-016-0505-0

Anderson, N. J., Heathcote, A. J., Engstrom, D. R., Ryves, D. B., Mills, K., Prairie, Y. T., et al. (2020). Anthropogenic alteration of nutrient supply increases the global freshwater carbon sink. *Science Advances*, *6*(16), eaaw2145. https://doi.org/10.1126/sciadv.aaw2145

Baliña, S., Sánchez, M. L., Izaguirre, I., & del Giorgio, P. A. (2023). Shallow lakes under alternative states differ in the dominant greenhouse gas emission pathways. *Limnology & Oceanography*, *68*(1), 1–13. https://doi.org/10.1002/lno.12243

Barton, K. (2020). *MuMin*: Multi-model inference. R package version 1.43.17. Retrieved from https://cran.r-project.org/package=MuMIn

Bastviken, D., Cole, J. J., Pace, M. L., & Van de-Bogert, M. C. (2008). Fates of methane from different lake habitats: Connecting whole-lake budgets and CH_4 emissions. *Journal of Geophysical Research*, *113*(2), 1–13. https://doi.org/10.1029/2007JG000608

Bates, D., Maechler, M., Bolker, B., & Walker, S. (2015). Fitting linear mixed-effects models using *lme4*. *Journal of Statistical Software*, *67*, 1–48. https://doi.org/10.1126/science.1176170

Burnham, K., & Anderson, D. (2002). *Model selection and multimodel inference: A practical information-theoretic approach*. Springer. https://doi.org/10.1007/b97636

Canadell, J. G., Monteiro, P. M. S., Costa, M., Cotrim da Cunha, L., Cox, P., Eliseev, A., et al. (2021). Global carbon and other biogeochemical cycles and feedbacks. In V. Masson-Delmotte, P. Zhai, A. Pirani, S. Connors, C. Péan, S. Berger, et al. (Eds.), *Climate change 2021: The physical science basis. Contribution of working group I to the sixth assessment report of the intergovernmental panel on climate change* (pp. 673–816). Cambridge University Press. https://doi.org/10.1017/9781009157896.007.674

Dacey, J. W. H., & Klug, M. J. (1979). Methane efflux from lake sediments through water lilies. *Science*, *203*(4386), 1253–1255. https://doi.org/10.1126/science.203.4386.1253

Davidson, T. A., Audet, J., Jeppesen, E., Landkildehus, F., Lauridsen, T. L., Søndergaard, M., & Syväranta, J. (2018). Synergy between nutrients and warming enhances methane ebullition from experimental lakes. *Nature Climate Change*, *8*(2), 156–160. https://doi.org/10.1038/s41558-017-0063-z

Deemer, B. R., & Holgerson, M. A. (2021). Drivers of methane flux differ between lakes and reservoirs, complicating global upscaling efforts. *Journal of Geophysical Research: Biogeosciences*, *126*(4), 1–15. https://doi.org/10.1029/2019JG005600

DelSontro, T., Boutet, L., St-Pierre, A., del Giorgio, P. A., & Prairie, Y. T. (2016). Methane ebullition and diffusion from northern ponds and lakes regulated by the interaction between temperature and system productivity. *Limnology & Oceanography*, *61*(S1), S62–S77. https://doi.org/10.1002/lno.10335

Downing, J. A. (2010). Emerging global role of small lakes and ponds: Little things mean a lot. *Limnética*, *29*(1), 9–24. https://doi.org/10.23818/limn.29.02

Downing, J. A., Cole, J. J., Middelburg, J. J., Striegl, R. G., Duarte, C. M., Kortelainen, P., et al. (2008). Sediment organic carbon burial in agriculturally eutrophic impoundments over the last century. *Global Biogeochemical Cycles*, *22*(1), GB1018. https://doi.org/10.1029/2006GB002854

Eugster, W., Kling, G., Jonas, T., McFadden, J. P., Wüest, A., MacIntyre, S., & Chapin, F. S., III. (2003). CO_2 exchange between air and water in an Arctic Alaskan and midlatitude Swiss lake: Importance of convective mixing. *Journal of Geophysical Research*, *108*(D12), 4362. https://doi.org/10.1029/2002jd002653

FAO. (2020). The state of world fisheries and aquaculture 2020: Sustainability in action. https://www.fao.org/3/ca9229en/CA9229EN.pdf
Hofmann, H. (2013). Spatiotemporal distribution patterns of dissolved methane in lakes: How accurate are the current estimations of the diffusive flux path? *Geophysical Research Letters*, *40*(11), 2779–2784. https://doi.org/10.1002/grl.50453
Holgerson, M. A., Ray, N. E., & Russ, C. (2023). High rates of carbon burial linked to autochthonous production in artificial ponds. *Limnology and Oceanography Letters*. https://doi.org/10.1002/lol2.10351
Holgerson, M. A., & Raymond, P. A. (2016). Large contribution to inland water CO_2 and CH_4 emissions from very small ponds. *Nature Geoscience*, *9*(3), 222–226. https://doi.org/10.1038/ngeo2654
Holgerson, M. A., Richardson, D. C., Roith, J., Bortolotti, L. E., Finlay, K., Hornbach, D. J., et al. (2022). Classifying mixing regimes in ponds and shallow lakes. *Water Resources Research*, *58*(7), e2022WR032522. https://doi.org/10.1029/2022WR032522
Jane, S. F., Mincer, J. L., Lau, M. P., Lewis, A. S. L., Stetler, J. T., & Rose, K. C. (2023). Longer duration of seasonal stratification contributes to widespread increases in lake hypoxia and anoxia. *Global Change Biology*, *29*(4), 1009–1023. https://doi.org/10.1111/gcb.16525
Jansen, J., Woolway, R. I., Kraemer, B. M., Albergel, C., Bastviken, D., Weyhenmeyer, G. A., et al. (2022). Global increase in methane production under future warming of lake bottom waters. *Global Change Biology*, *28*(18), 5427–5440. https://doi.org/10.1111/gcb.16298
Lenth, R. (2018). *emmeans*: Estimated marginal means, aka least-squares means. R package version 1.2.3.
MacIntyre, S., Sickman, J. O., Goldthwait, S. A., & Kling, G. W. (2006). Physical pathways of nutrient supply in a small, ultraoligotrophic arctic lake during summer stratification. *Limnology & Oceanography*, *51*(2), 1107–1124. https://doi.org/10.4319/lo.2006.51.2.1107
Malerba, M. E., de Kluyver, T., Wright, N., Schuster, L., & Macreadie, P. I. (2022). Methane emissions from agricultural ponds are underestimated in national greenhouse gas inventories. *Communications Earth and Environment*, *3*(1), 306. https://doi.org/10.1038/s43247-022-00638-9
Natchimuthu, S., Panneer Selvam, B., & Bastviken, D. (2014). Influence of weather variables on methane and carbon dioxide flux from a shallow pond. *Biogeochemistry*, *119*(1–3), 403–413. https://doi.org/10.1007/s10533-014-9976-z
Ozimek, T., van Donk, E., & Gulati, R. D. (1993). Growth and nutrient uptake by two species of *Elodea* in experimental conditions and their role in nutrient accumulation in a macrophyte-dominated lake. *Hydrobiologia*, *251*(1–3), 13–18. https://doi.org/10.1007/bf00007159
Pieczyńska, E. (1993). Detritus and nutrient dynamics in the shore zone of lakes: A review. *Hydrobiologia*, *251*(1–3), 49–58. https://doi.org/10.1007/bf00007164
Prairie, Y. T. (1996). Evaluating the predictive power of regression models. *Canadian Journal of Fisheries and Aquatic Sciences*, *53*(3), 490–492. https://doi.org/10.1139/f95-204
Ray, N. E., & Fulweiler, R. W. (2021). Negligible greenhouse gas release from sediments in oyster habitats. *Environmental Science and Technology*, *55*(20), 14225–14233. https://doi.org/10.1021/acs.est.1c05253
Ray, N. E., Holgerson, M. A., Andersen, M. R., Bikše, J., Bortolotti, L. E., Futter, M., et al. (2023). Spatial and temporal variability in summertime dissolved carbon dioxide and methane in temperate ponds and shallow lakes. *Limnology and Oceanography*, *68*(7), 1530–1545. https://doi.org/10.1002/lno.12362
Raymond, P. A., Hartmann, J., Lauerwald, R., Sobek, S., McDonald, C., Hoover, M., et al. (2013). Global carbon dioxide emissions from inland waters. *Nature*, *503*(7476), 355–359. https://doi.org/10.1038/nature12760
Read, J. S., Hamilton, D. P., Jones, I. D., Muraoka, K., Winslow, L. A., Kroiss, R., et al. (2011). Derivation of lake mixing and stratification indices from high-resolution lake buoy data. *Environmental Modelling & Software*, *26*(11), 1325–1336. https://doi.org/10.1016/j.envsoft.2011.05.006
Renwick, W. H., Sleezer, R. O., Buddemeier, R. W., & Smith, S. V. (2006). Small artificial ponds in the United States: Impacts on sedimentation and carbon budget. In *Proceedings of the eighth federal interagency sedimentation conference (8thFISC), April 2-6, 2006*. https://pubs.usgs.gov/misc/FISC_1947-2006/pdf/1st-7thFISCs-CD/8thFISC/Session%2010A-3_Renwick.pdf
Riera, J. L., Schindler, J. E., & Kratz, T. K. (1999). Seasonal dynamics of carbon dioxide and methane in two clear-water lakes and two bog lakes in northern Wisconsin, U.S.A. *Canadian Journal of Fisheries and Aquatic Sciences*, *56*(2), 265–274. https://doi.org/10.1139/f98-182
Rosentreter, J. A., Borges, A. V., Deemer, B. R., Holgerson, M. A., Liu, S., Song, C., et al. (2021). Half of global methane emissions come from highly variable aquatic ecosystem sources. *Nature Geoscience*, *14*(4), 225–230. https://doi.org/10.1038/s41561-021-00715-2
Signorell, A., Aho, K., Alfons, A., Anderegg, N., Aragon, T., Arppe, A., et al. (2017). *DescTools*: Tools for descriptive statistics. R package version 0.99 (Vol. *28*, p. 17).
Sinclair, J. S., Reisinger, A. J., Bean, E., Adams, C. R., Reisinger, L. S., & Iannone, B. V. (2020). Stormwater ponds: An overlooked but plentiful urban designer ecosystem provides invasive plant habitat in a subtropical region (Florida, USA). *Science of the Total Environment*, *711*, 135133. https://doi.org/10.1016/j.scitotenv.2019.135133
Søndergaard, M., Nielsen, A., Skov, C., Baktoft, H., Reitzel, K., Kragh, T., & Davidson, T. A. (2023). Temporarily and frequently occurring summer stratification and its effects on nutrient dynamics, greenhouse gas emission and fish habitat use: Case study from Lake Ormstrup (Denmark). *Hydrobiologia*, *850*(1), 65–79. https://doi.org/10.1007/s10750-022-05039-9
Taylor, S., Gilbert, P. J., Cooke, D. A., Deary, M. E., & Jeffries, M. J. (2019). High carbon burial rates by small ponds in the landscape. *Frontiers in Ecology and the Environment*, *17*(1), 25–31. https://doi.org/10.1002/fee.1988
Tian, H., Xu, R., Canadell, J. G., Thompson, R. L., Winiwarter, W., Suntharalingam, P., et al. (2020). A comprehensive quantification of global nitrous oxide sources and sinks. *Nature*, *586*(7828), 248–256. https://doi.org/10.1038/s41586-020-2780-0
Vachon, D., Langenegger, T., Donis, D., Beaubien, S. E., & McGinnis, D. F. (2020). Methane emission offsets carbon dioxide uptake in a small productive lake. *Limnology and Oceanography Letters*, *5*(6), 384–392. https://doi.org/10.1002/lol2.10161
van Bergen, T. J. H. M., Barros, N., Mendonça, R., Aben, R. C. H., Althuizen, I. H. J., Huszar, V., et al. (2019). Seasonal and diel variation in greenhouse gas emissions from an urban pond and its major drivers. *Limnology & Oceanography*, *64*(5), 2129–2139. https://doi.org/10.1002/lno.11173
Waldo, S., Beaulieu, J. J., Barnett, W., Balz, D. A., Vanni, M. J., Williamson, T., & Walker, J. T. (2021). Temporal trends in methane emissions from a small eutrophic reservoir: The key role of a spring burst. *Biogeosciences*, *18*(19), 5291–5311. https://doi.org/10.5194/bg-18-5291-2021
Wik, M., Crill, P. M., Varner, R. K., & Bastviken, D. (2013). Multiyear measurements of ebullitive methane flux from three subarctic lakes. *Journal of Geophysical Research: Biogeosciences*, *118*(3), 1307–1321. https://doi.org/10.1002/jgrg.20103
Wik, M., Thornton, B. F., Bastviken, D., Uhlbäck, J., & Crill, P. M. (2016). Biased sampling of methane release from northern lakes: A problem for extrapolation. *Geophysical Research Letters*, *43*(3), 1256–1262. https://doi.org/10.1002/2015GL066501.Received
Wik, M., Thorton, B. F., Bastviken, D., MacIntyre, S., Varner, R. K., & Crill, P. M. (2014). Energy input is primary controller of methane bubbling in subarctic lakes. *Geophysical Research Letters*, *41*(2), 555–560. https://doi.org/10.1002/2013GL058510.Received
Wik, M., Varner, R. K., Anthony, K. W., MacIntyre, S., & Bastviken, D. (2016b). Climate-sensitive northern lakes and ponds are critical components of methane release. *Nature Geoscience*, *9*(2), 99–105. https://doi.org/10.1038/ngeo2578

Woolway, R. I., Merchant, C. J., Van Den Hoek, J., Azorin-Molina, C., Nõges, P., Laas, A., et al. (2019). Northern hemisphere atmospheric stilling accelerates lake thermal responses to a warming world. *Geophysical Research Letters*, *46*(21), 11983–11992. https://doi.org/10.1029/2019GL082752

Yentsch, C., & Menzel, D. (1963). A method for the determination of phytoplankton chlorophyll and phaeophytin by fluorescence. *Deep-Sea Research and Oceanographic Abstracts*, *10*(3), 221–231. https://doi.org/10.1016/0011-7471(63)90358-9